科学通报 2025 年 第 70 卷 第 22 期: 3722 ~ 3734
自然科学基金项目进展专栏 评 述
《中国科学》杂志社 SCIENCE CHINA PRESS

离子液体介导的钙钛矿光伏电池

杨宛, 顾子涵, 晁凌锋*, 夏英东*, 陈永华*

南京工业大学柔性电子(未来技术)学院, 先进材料研究院, 南京 210000

* 联系人, E-mail: iamlfchao@njtech.edu.cn; iamydxia@njtech.edu.cn; iamyhchen@njtech.edu.cn

2024-12-12 收稿, 2025-01-22 修回, 2025-02-08 接受, 2025-02-10 网络版发表

国家杰出青年科学基金(22425903)、国家自然科学基金(U24A20568, 61705102, 62288102, 22409091, 22409090, 62205142)、国家重点研发计划(2023YFB4204500, 2020YFA07099003)和江苏省自然科学基金(BK20241875, BE2022023, BK20220010, BZ2023060)资助

摘要 离子液体(ionic liquids, ILs)是一类在室温下为液态的盐类, 因其独特的物理和化学性质, 在钙钛矿太阳能电池(perovskite solar cells, PSCs)领域展现出广泛的应用潜力. 尤其是, ILs在提高PSCs的性能和稳定性方面扮演了重要角色. 本文系统总结了离子液体作为溶剂的钙钛矿太阳能电池研究进展, 重点关注ILs在PSCs制备中的关键功能, 并提出了一系列策略来优化和增强ILs在PSCs中的应用, 包括界面工程、溶剂工程和添加剂工程. 接着, 就ILs制备$FAPbI_3$ (FA, 甲脒)钙钛矿、二维钙钛矿、全无机钙钛矿以及钙钛矿的大规模生产提出了我们的观点. 此外, 我们还揭示了ILs实现高稳定和高效率PSCs的潜在机制. 最后, 从大规模生产和技术的角度出发, 讨论了ILs基PSCs面临的挑战和未来的研究方向, 为PSCs的商业化进程提供了新的视角和方法.

关键词 钙钛矿太阳能电池, 离子液体, 稳定性, 大面积制备

钙钛矿太阳能电池(perovskite solar cells, PSCs)由于优异的光电性能、与溶液处理的兼容性和低廉的制造成本, 被视为未来商业化最有前景的下一代光伏技术之一[1~3]. 到目前为止, PSCs的功率转换效率(power conversion efficiency, PCE)已经突破26%[4]. 与传统的硅基和其他光伏技术相比, PSCs的主要竞争优势在于可通过简单的溶液法制备薄膜. 其中, 有机溶剂在溶液法制备钙钛矿光伏器件中发挥着重要作用, 溶剂的性质显著影响着前驱体溶液的化学环境、结晶动力学以及钙钛矿膜形貌和质量[5,6].

目前, 高质量钙钛矿薄膜的制备通常使用*N*,*N*-二甲基甲酰胺(DMF)、二甲亚砜(DMSO)、*N*-甲基吡咯烷酮(NMP)等作为单一溶剂或混合溶剂[7~10]. 这些沸点较高且配位能力强的溶剂与钙钛矿前驱体之间存在强相互作用, 导致溶剂在薄膜沉积过程中难以蒸发. 因此, 为了获得高质量的钙钛矿薄膜, 通常需要借助反溶剂辅助结晶的方法[11,12]. 然而, 溶剂本身的毒理学问题和繁琐的反溶剂工程需要更高的操作技术和环境要求, 严重阻碍着PSCs的商业化进程[13,14]. 因此, 开发一种绿色无污染、工艺简单、高效、稳定、低成本的新型溶剂, 对于在实验室和工业规模上制备有机-无机杂化钙钛矿材料和器件至关重要.

离子液体(ionic liquids, ILs)是一类在室温下呈液态的熔盐[15], 由多种有机阳离子(如咪唑鎓、吡咯烷鎓、三唑鎓、吡啶鎓、哌啶鎓、铵和鏻)和有机或无机阴离子(如卤化物、四氟硼酸根、六氟磷酸根、磷酸根、羧酸、磺酸和酰亚胺)组成, 如图1所示. 这些化合物因其熔点低、蒸汽压小、酸度可调、溶解度高、载流子迁移率高、优异的热稳定性和环境友好性等[16,17]独特的物理化学性质, 在化学合成、电化学、分离技术等领域展现出显著的应用潜力. 特别是在钙钛矿太阳能电池领域, ILs得到了广泛的关注和研究[18,19], 并已展现出显著提升效率和稳定性的巨大潜力.

引用格式: 杨宛, 顾子涵, 晁凌锋, 等. 离子液体介导的钙钛矿光伏电池. 科学通报, 2025, 70: 3722–3734
Yang W, Gu Z, Chao L, et al. Ionic liquids mediated perovskite photovoltaic cells (in Chinese). Chin Sci Bull, 2025, 70: 3722–3734, doi: 10.1360/TB-2024-1310

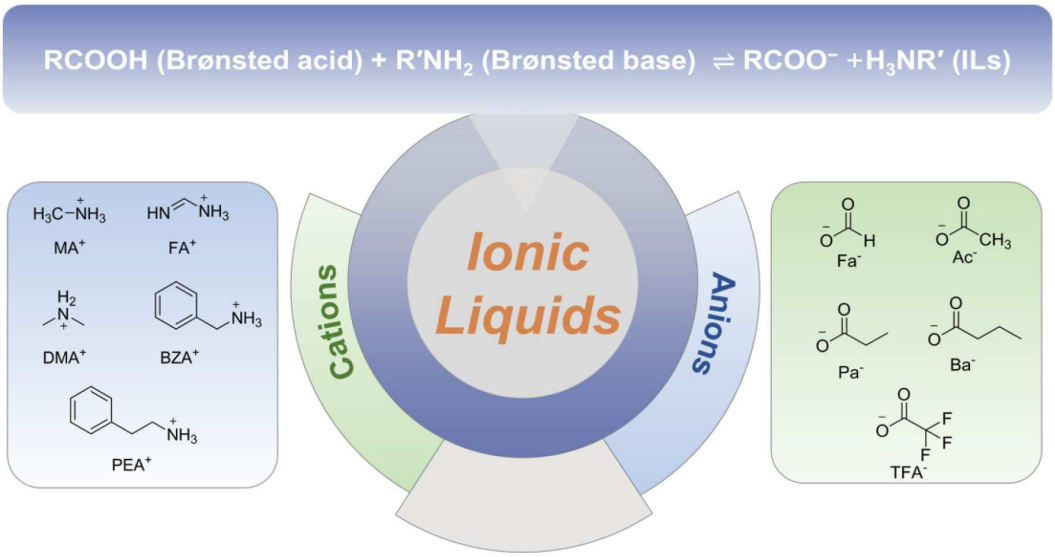

图 1 (网络版彩色)PSCs领域常见离子液体的一些阳离子和阴离子的结构
Figure 1 (Color online) Structures of some common cations and anions of ILs in the perovskite solar cell field

本文重点介绍了ILs在PSCs方面的应用，例如醋酸甲胺(MAAc)、甲酸甲胺(MAFa)和醋酸正丁胺(BAAc)，探索了利用ILs制备钙钛矿薄膜的方法，并就ILs制备全无机钙钛矿、二维钙钛矿、$FAPbI_3$钙钛矿以及大面积制备进行了总结. 我们还揭示了ILs实现高性能PSCs的机制，从大规模生产和技术角度系统地讨论了基于ILs的PSCs的挑战和未来方向.

1 离子液体在PSCs中的应用

2015年, Moore等人[20]首次报道了一种环境友好型离子液体MAFa作为前驱体溶剂，可以在不经历中间相的情况下制备出高质量钙钛矿薄膜[21]. 这为ILs作为钙钛矿前驱体的溶剂打开了大门. 然而，这种钙钛矿薄膜未被制备成钙钛矿太阳能电池.

2019年, 我们团队[22]报道了一种ILs MAAc作为钙钛矿前驱体溶剂，可以在空气中通过一步法制备PSCs. MAAc通过形成Pb-O配位和N-H···I氢键来溶解钙钛矿前驱体，这与常用的有机分子溶剂不同[23]，如图2(a)所示. 同时，这种强的相互作用能够调控钙钛矿前驱体溶液的总胶体浓度，使胶体粒径分布均匀，如图2(b)所示. 基于此，通过简单的旋涂方法可以在空气中制备出晶粒均匀且无杂质的优异钙钛矿薄膜，实现了20%的PCE，这是当时空气中一步法旋涂制备PSCs的最高PCE之一. 在此基础上，进一步通过添加剂工程[23]、溶剂工程[24]和界面工程[25,26]将效率提高到22%以上[23]. 此外，简单且环保的制备方法适合大规模生产工艺，例如刮刀涂布[27]、狭缝涂布[28]、喷墨印刷[29]等. 最重要的是，钙钛矿器件在没有进一步钝化的情况下就展现出了优异的稳定性，包括在70%湿度条件下长达200 h的耐湿性、在85°C下1000 h的热稳定性，以及在最大功率点下500 h的运行稳定性.

2020年，Wang等人[30]利用MAAc溶剂成功在环境空气中制备了高效稳定的全无机钙钛矿. 在前驱体溶液中，MAAc通过羰基与PbI_2的强相互作用以及胺基与碘离子之间形成的氢键，增强了前驱体溶液的稳定性，有效防止了溶液的氧化，如图2(c)所示. 在成膜过程中，MAAc通过与溶质的相互作用延缓结晶，促进了均匀、大尺寸晶粒的高质量钙钛矿薄膜形成，如图2(d)所示. 最终，采用该策略制备的全无机PSCs ($CsPbI_{2.5}Br_{0.5}$)达到了17.10%的PCE，并且在连续光照下展示了超过1500 h的长期稳定性，如图2(e)所示. 这项研究克服了全无机钙钛矿材料的稳定性挑战，为推动其商业化进程提供了重要的技术支撑[31,32]. 2022年，Meng等人[33]报道了一种新型离子液体醋酸二甲胺(DMAAc)作为钙钛矿前驱体的溶剂，通过均匀化中间相分布来调节结晶过程，从而获得高质量的$CsPbI_3$薄膜最终，实现了1.25 V的高开路电压和大于21%的PCE，这是迄今为止报道的最高纪录.

此外，离子液体对制备非卤化物铅源的PSCs也发挥着重要作用[34,35]. Chen等人[36]发现离子液体MAAc

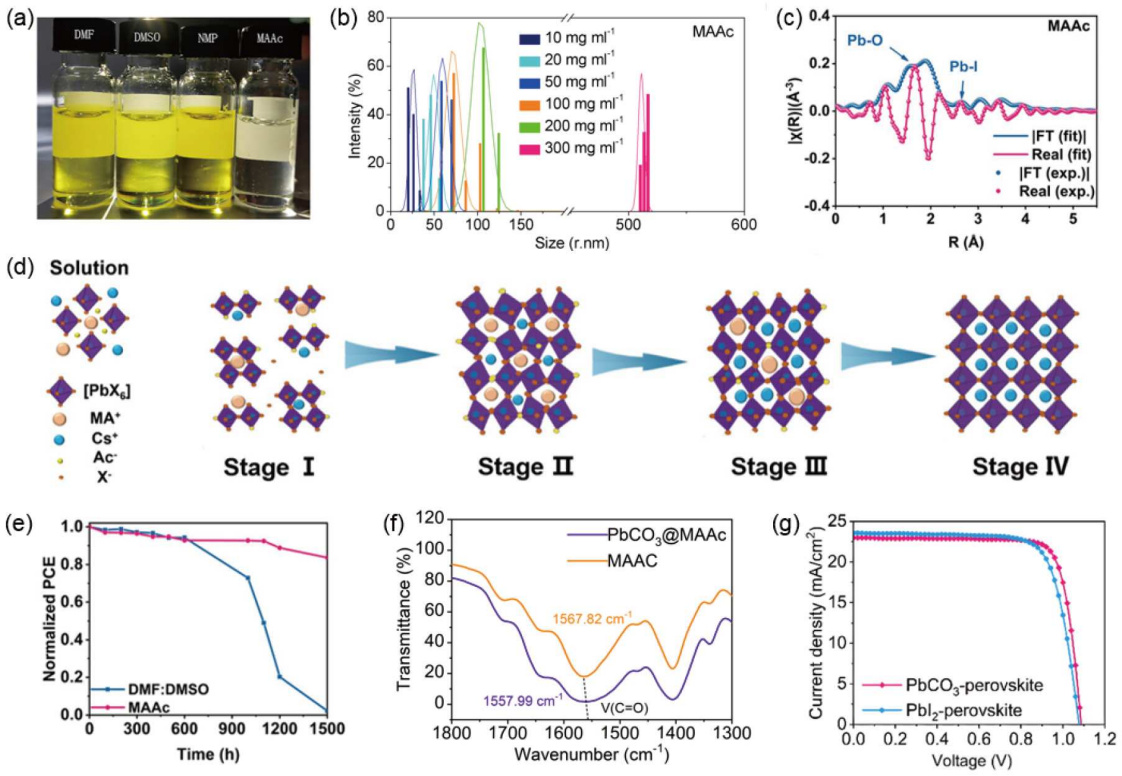

图 2 (网络版彩色)MAAc作为钙钛矿前驱体溶剂的应用. (a) 基于不同溶剂的钙钛矿前驱体溶液的图片; (b) 动态光散射(DLS)光谱显示基于MAAc的钙钛矿前驱体溶液胶束[22]; (c) 基于MAAc的Pb L3-edge XAFS光谱; (d) $CsPbI_2Br$薄膜结晶动力学; (e) 基于不同溶剂的未封装$CsPbI_2Br$器件的长期运行稳定性[30]; (f) MAAc溶剂和$PbCO_3$@MAAc溶液的FTIR光谱; (g) 基于$PbCO_3$和PbI_2钙钛矿器件的*J-V*曲线[36]

Figure 2 (Color online) The application of MAAc as a solvent for perovskite precursors. (a) Picture of perovskite precursor solutions based on different solvents; (b) dynamic light scattering (DLS) spectra show the micelles of MAAc-based perovskite precursor solutions[22]; (c) the Pb L3-edge of MAAc was studied through XAFS spectra; (d) $CsPbI_2Br$ film crystallization kinetics; (e) long-term operational stability of the unencapsulated $CsPbI_2Br$ devices with MAAc and DMF:DMSO films[30]; (f) the FTIR spectra of MAAc solvent and $PbCO_3$@MAAc solution, respectively; (g) *J-V* curves of the perovskite devices based on $PbCO_3$ and PbI_2[36]

能有效溶解非卤化物铅盐, 并通过与Pb^{2+}形成强配位和氢键作用, 形成稳定的钙钛矿前驱体溶液, 如图2(f)所示. 在没有任何添加剂和钝化剂的情况下, 基于$PbSO_4$、$PbAc_2$和$PbCO_3$的PSCs的PCE分别达到14.48%、19.21%和20.13%, 如图2(g)所示.

2 MAAc用于无电子传输层的钙钛矿太阳能电池

PSCs通常需要电子提取层和空穴提取层来实现有效的电荷提取和传输. 低成本且无电荷传输层(charge transport layer, CTL)的简化钙钛矿器件引起了广泛关注[37]. 改进无CTL器件的关键取决于钙钛矿/电极界面的能级匹配. 为了解决这个问题, 必须在界面处引入额外的修饰层[38]. 虽然性能得到了提高, 但牺牲了无CTL PSCs的结构的简单性.

2020年, Li等人[39]使用MAAc作为溶剂, 无需额外的界面修饰即可实现高效稳定的无电子传输层(electron transport layer, ETL)钙钛矿太阳能电池, 如图3(a)所示. 在成膜过程中, MAAc可以原位物理吸附到ITO表面形成偶极子层, 有效降低了ITO的功函数, 导致原位能带弯曲, 加速了界面处的电荷提取, 如图3(b)所示. 此外, 经MAAc处理的无ETL钙钛矿薄膜结晶质量也得到了明显改善, 如图3(c)所示. 最终, 基于该策略制备的无ETL器件的PCE为21.08%, 这是无ETL PSCs中最高的报道, 如图3(d)所示. 与其他工艺相比, 基于MAAc无ETL的PSCs器件具有出色的稳定性, 在连续光照400 h下仍能保持原PCE的80%以上, 如图3(e)所示. 在这项工作中, 利用离子液体溶剂制备无ETL的PSCs, 可以实现从工艺到器件结构的简化, 为实现高效稳定的简化器件提供了新途径. 此外, ILs的可设计性允许以更高

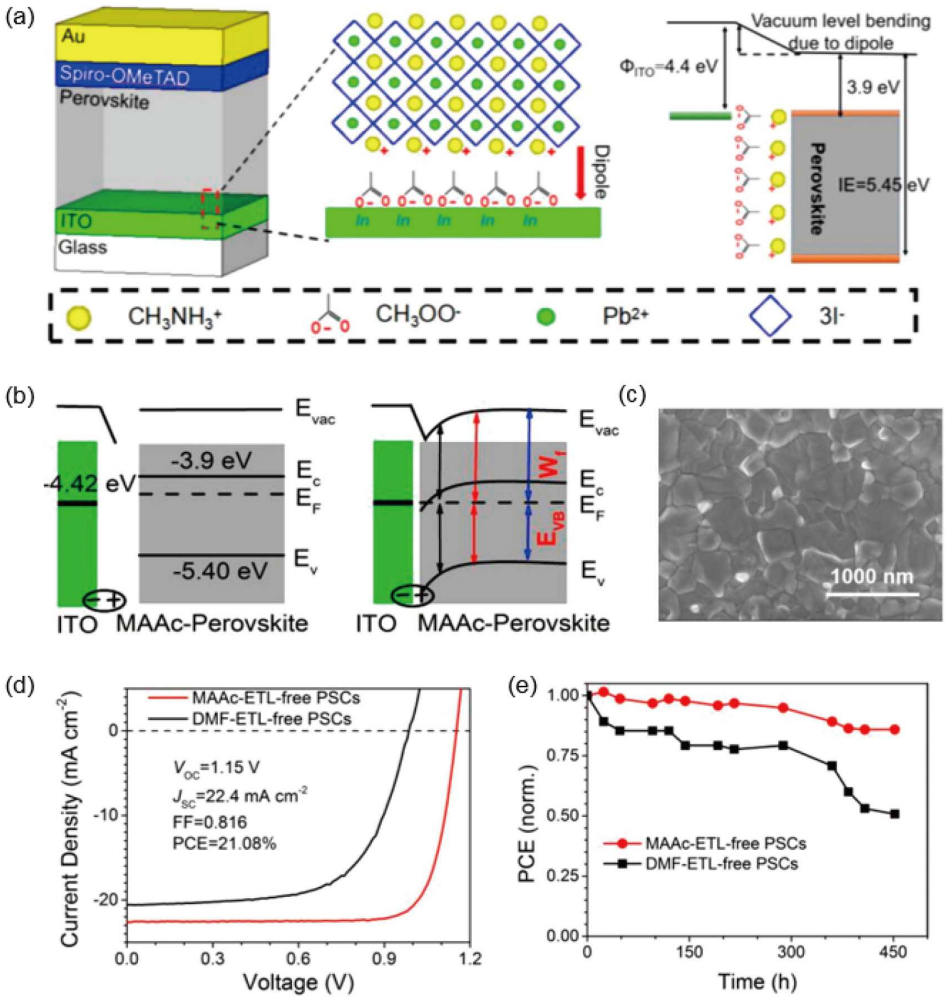

图 3 (网络版彩色)MAAc制备无电子传输层的钙钛矿太阳能电池. (a) 无ETL钙钛矿太阳能电池的器件结构; (b) ITO/MAAc-钙钛矿异质结; (c) 基于MAAc溶剂的无ETL钙钛矿薄膜的SEM图像; (d) 基于DMF和MAAc的无ETL PSCs的*J-V*特性; (e) 在惰性环境中使用不同溶剂的PSCs器件的光稳定性[39]

Figure 3 (Color online) MAAc-prepared perovskite solar cells without an electron transport layer. (a) Device structure of the ETL-free perovskite solar cell; (b) ITO/MAAc-perovskite heterojunction; (c) SEM top-view images of MAAc-ETL-free perovskite films; (d) *J-V* characteristics for the DMF- and MAAc-ETL-free PSCs; (e) the photostability of PSCs devices with different solvents in an inert environment[39]

的效率制备简化的钙钛矿器件. 例如, 阳离子的结构可以改变为共轭结构, 有利于电子的传递. 还可以设计和合成具有特殊官能团的ILs, 控制和改变分子的堆叠方式, 以达到最佳的电荷转移.

3 ILs制备二维层状钙钛矿

MAAc不仅能够制备包括不同胺盐(例如MAX和FAX)和铅源(例如PbI_2、$PbBr_2$和$PbCl_2$)在内的一系列三维(3D)钙钛矿, 而且在二维(2D)层状钙钛矿太阳能电池的研究领域也展现出了卓越的性能[40~43], 包括Ruddlesden-Popper (RP)相和Dion-Jacobson (DJ)相.

Ren等人[43]通过在前驱体溶液中引入2-(甲硫基)乙胺盐酸盐(MTEACl), 成功制备出2DRP层状钙钛矿. 2D $(MTEA)_2(MA)_4Pb_5I_{16}$层状钙钛矿中的两个MTEA分子通过S-S键增强相互作用力, 极大地提高了钙钛矿骨架的稳定性, 如图4(a), (b)所示. 此外, 薄膜显示出更好地垂直于基底方向的优先生长, 这有利于载流子的提取和传输. 良好的晶体可以有效降低薄膜缺陷态密度, 如图4(c)所示. 最终, 基于MTEACl的2DRP薄膜获得了18.06%的PCE(认证值为17.80%), 这是基于2DRP PSCs中报道的最佳效率之一, 如图4(d)所示. 最重要的是, 2D层状钙钛矿薄膜和器件在光、热和最大功率跟踪下

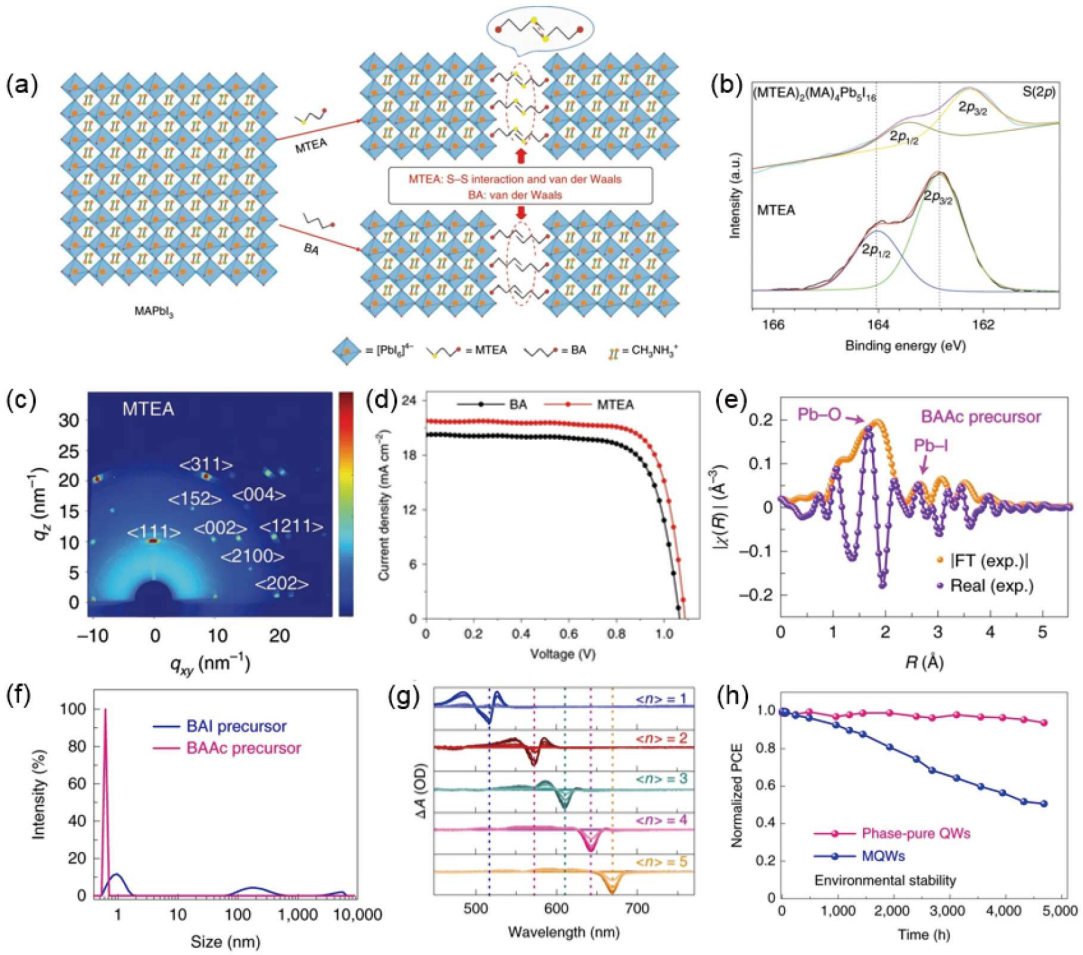

图 4 (网络版彩色)ILs在二维层状钙钛矿方面的应用. (a) 基于MTEA和BA间隔分子的2DRP钙钛矿晶体结构示意图; (b) MTEACl薄膜和$(MTEA)_2(MA)_4Pb_5I_{16}$钙钛矿薄膜的X射线光电子能谱中的S(2p)图像; (c) $(MTEA)_2(MA)_4Pb_5I_{16}$钙钛矿薄膜的GIWAXS图案; (d) $(MTEA)_2(MA)_4Pb_5I_{16}$和$(BA)_2(MA)_4Pb_5I_{16}$ 2DRP钙钛矿器件的*J-V*曲线[43]; (e) 基于BAAc钙钛矿前驱体溶液的扩展X射线吸收精细结构光谱; (f) BAI和BAAc基钙钛矿前驱体溶液的粒径分布图; (g) 具有不同阱宽度(n)的纯相QW薄膜的吸收(ΔA)光谱; (h) 器件在连续光照下的稳定性[49]

Figure 4 (Color online) Applications of ionic liquids in two-dimensional layered perovskites. (a) Schematic diagram of the crystal structure of 2DRP perovskite based on MTEA and BA spacer molecules; (b) a comparison of X-ray photoelectron spectroscopy spectra (XPS) of the S(2p) of the MTEACl and $(MTEA)_2(MA)_4Pb_5I_{16}$ films; (c) GIWAXS patterns for the $(MTEA)_2(MA)_4Pb_5I_{16}$ perovskite films; (d) *J-V* curves for devices based on $(MTEA)_2(MA)_4Pb_5I_{16}$ and $(BA)_2(MA)_4Pb_5I_{16}$ 2DRP perovskites[43]; (e) extended X-ray absorption fine structure spectrum based on BAAc perovskite precursor solution; (f) particle size distribution diagrams of BAI and BAAc-based perovskite precursor solutions; (g) chirp-corrected photo-induced changes in absorption (ΔA) spectra of the phase-pure QW films with varied average well width (n); (h) the stability of the device under continuous light illumination[49]

展现出卓越的稳定性. Niu等人[44]将$BDAMA_4Pb_5I_{16}$ (1,4-butanediamine, BDA)作为DJ相PSCs的光活性层, 通过调整量子阱的势垒厚度, 实现了DJ相钙钛矿17.91%的效率. 这项工作为构建高效稳定的2D层状PSCs提供了新的思路, 并且为混合钙钛矿类材料的潜在应用提供了可能性. 此外, MAAc也可以作为溶剂来制备二维层状锡(Sn)基钙钛矿(例如$BA_2MA_3Sn_4I_{13}$), 这得益于Ac^-和Sn^{2+}之间的强相互作用[45]. 通过这种方法可以获得具有大尺寸晶粒的钙钛矿薄膜, 并实现了PCE为4.03%的钙钛矿太阳能电池, 这是当时Sn基钙钛矿太阳能电池的最好性能之一.

然而, 由于形成能接近, 二维层状钙钛矿往往会形成具有随机阱宽度分布的多量子阱(multiple quantum well, MQW)结构, 这严重阻碍了该领域的进一步进展, 特别是对于深入研究2D钙钛矿材料的各种物理化学性质[46~48]. 因此, 制备纯相2D钙钛矿薄膜至关重要. 为了解决这个问题, Liang等人[49]首次通过引入一种新型离子液体醋酸丁胺(BAAc)替代传统的丁胺氢碘酸盐

(BAI), 成功制备出纯相二维层状钙钛矿薄膜. BAAc通过配位和氢键与前驱体溶液中的溶质相互作用, 如图4(e)所示. 强化学作用可以防止胶体颗粒聚集并促进其均匀分散[50], 如图4(f)所示. 前驱体溶液中胶体颗粒的窄尺寸分布倾向于接近单分散晶胞颗粒, 有利于形成相纯的QW薄膜. 在薄膜形成过程中, 中间相$(BA)_2(MA)_3Pb_4I_{13-x}Ac_x$, $(MAI)_2$ ($x\leqslant 2$)能够随着其他溶剂的蒸发而凝胶化. 中间相中不稳定的Ac^-离子与I^-发生交换, 与MA^+结合形成容易分解的MAAc并蒸发, 最终形成相纯的QW薄膜, 如图4(g)所示. 最终, 钙钛矿光伏器件得到16.25%的光电转换效率以及1.31 V的高开路电压. 而且, 纯相钙钛矿薄膜中的无机层受到均匀间隔层的保护, 可以大大提高钙钛矿的稳定性. 尤其是在环境空气中保存4680 h后, 仍保持原PCE的93.8%, 如图4(h)示. 这是首次报道具有优异稳定性、独特结构和光电性能的纯相QW薄膜, 对于研究层状钙钛矿材料的各种物理和化学性质至关重要.

4 ILs用于黑相α-$FAPbI_3$ PSCs

α-$FAPbI_3$因其高载流子迁移率、优异的热稳定性以及1.48 eV的带隙, 被认为是最接近Shockley-Queisser极限的钙钛矿太阳能电池材料[51]. 然而, 由于FA^+离子的大尺寸引起的晶格畸变, α-$FAPbI_3$在室温条件下极易向非钙钛矿相(δ相)转变, 这一相变不仅损害了材料的稳定性, 也限制了其商业化进程[52].

2021年, Hui等人[53]使用ILs MAFa作为溶剂, 实现在环境空气中制备高效稳定的黑相α-$FAPbI_3$钙钛矿. MAFa通过氢键和配位作用改变了PbI_2的化学环境, 在前驱体溶液中形成螯合单元, 如图5(a)所示. 这种相互作用的强度比MAAc和PbI_2的弱. 在薄膜形成过程中, 化学作用诱导PbI_2晶体沿垂直方向规则生长, 如图5(b)所示. 值得注意的是, 由于MAFa的挥发, 垂直生长的PbI_2结构形成了许多纳米尺度的离子通道, 促进了FAI进入PbI_2薄膜, 从而在环境空气中快速而稳定地转化为α-$FAPbI_3$, 如图5(c)所示. 纳米离子通道的形成直接降低了α-$FAPbI_3$钙钛矿形成能垒, 这一策略加速了钙钛矿的相变, 使得钙钛矿能够在室温下实现相转变, 如图5(d)所示. 此外, 基于MAFa的$FAPbI_3$钙钛矿的最大优势在于其优异的稳定性. 器件在惰性气体中放置5000 h后保留了93%的原始PCE, 并在最大功率点下追踪500 h后仍然保留了90%的初始效率, 如图5(e)所示. 这种长期的稳定性归因于钙钛矿结构的完整性和较少的缺陷. 此外, 残留的MAFa能够锚定在晶界或表面, 有效防止钙钛矿的降解. 这一策略为高效且稳定的钙钛矿太阳能电池的工业化大规模生产铺平了道路.

最近, Chen等人[54]报道了一种通过离子液体MAAc溶剂在分子水平上调控前驱体溶液中胶体的性质, 实现α-$FAPbI_3$钙钛矿的直接且稳定相转变的策略. 研究发现, 乙酸根(Ac^-)与Pb^{2+}通过C=O···Pb配位作用产生较强的相互作用, 导致Pb-I键长变长, 这促进了FAI参与反应, 从而快速且稳定地转化为α-$FAPbI_3$, 如图5(f)所示. 最终器件达到了接近24%的效率, 这是当时空气中一步法制备PSCs且无需反溶剂处理的最高效率, 如图5(g)所示.

5 ILs用于全丝网印刷钙钛矿太阳能电池

丝网印刷技术被认为是简化、成本效益高、可靠且可扩展的全印刷钙钛矿太阳能电池工业化制造的良好候选方案[55~57]. 对于PSCs, 介孔支架(如m-TiO_2或m-ZrO_2)和碳电极可以很容易地丝网印刷到导电玻璃上, 这是构建PSCs最简单且成本最低的方法之一[58]. 然而, 由于钙钛矿油墨的低黏度和不稳定性, 通过丝网印刷制备钙钛矿薄膜仍然是一个挑战.

2022年, Chen等人[59]开发了一种离子液体MAAc作为溶剂的丝网印刷技术, 成功制备了高质量钙钛矿薄膜, 如图6(a)所示. 在退火过程中, 溶剂MAAc在空气-钙钛矿油墨-基材复合相的接触线边缘迅速蒸发, 钙钛矿溶质同时转移到接触线, 如图6(b)所示. 向上蒸发和向下沉积的协同作用导致接触线快速且逐步地穿过整个印刷区域, 从而在基板上形成连续的钙钛矿薄膜. 基于这种丝网印刷方法制备了致密且无针孔的钙钛矿薄膜, 平均晶粒尺寸超过600 nm, 如图6(c)所示. 离子液体MAAc的黏度对温度极其敏感, 这种特性使其作为钙钛矿溶剂时能显著增加墨水的黏度, 如图6(d)所示. 黏度赋予了墨水更强的凝聚力和对基底的黏附力, 从而提高了印刷质量. 由于MAAc的高黏度特性, 它限制了钙钛矿溶液的流动性, 从而有效抑制了MA^+/FA^+的去质子化过程, 防止了它们转化为挥发性的甲胺(MA)或甲脒(FA)[60]. 此外, MAAc中的质子胺和羧酸成分能够钝化整个油墨系统, 有助于延长钙钛矿油墨的老化时间以保持其稳定性[23]. 最终, 通过这种方法, 即使在环境空气中, 也能实现高达20.52%的光电转换效率, 如图6(e)所示. 此外, 在最大功率点运行300 h后, 初始效率保持了96.75%.

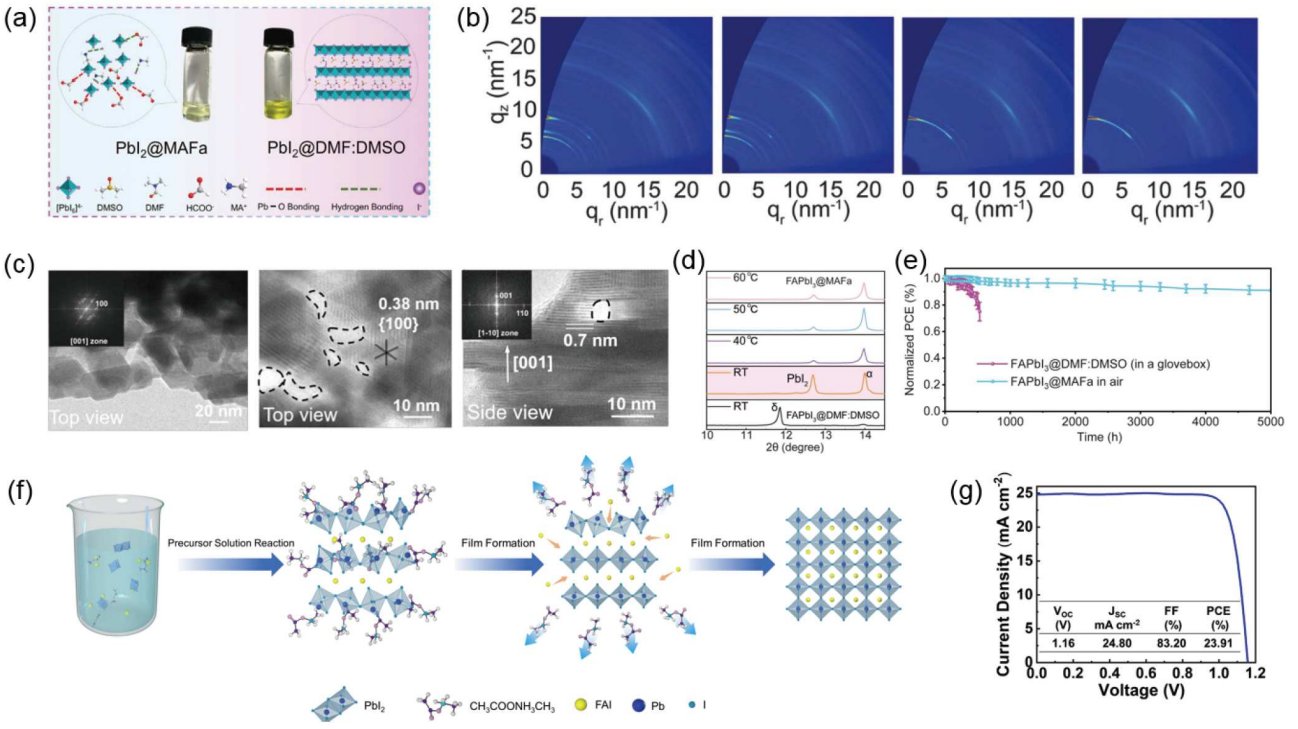

图 5 (网络版彩色)ILs用于制备α-$FAPbI_3$ PSCs. (a) PbI_2分别在MAFa和DMF@DMSO中的化学作用示意图; (b) PbI_2@MAFa薄膜在相应退火时间的原位GIWAXS谱图; (c) PbI_2@MAFa薄膜的HRTEM和相应的傅里叶变换俯视图和侧视图; (d) 不同溶剂体系下制备的$FAPbI_3$钙钛矿薄膜的XRD谱图; (e) 器件在惰性气体中的储存稳定性[53]; (f) $FAPbI_3$钙钛矿形成机制; (g) $FAPbI_3$ PSCs的*J-V*曲线[54]

Figure 5 (Color online) ILs for the fabrication of α-$FAPbI_3$ perovskite solar cells. (a) Schematic diagram of the chemical action of lead iodide in MAFa and DMF@DMSO, respectively; (b) *in situ* GIWAXS spectra of PbI_2@MAFa films at corresponding annealing time; (c) HRTEM and corresponding Fourier transform of PbI_2@MAFa thin films top view and side view; (d) $FAPbI_3$ perovskite films prepared under different solvent systems are characterized by XRD spectra; (e) storage stability in inert gas[53]; (f) mechanism of the $FAPbI_3$ perovskite formation process; (g) *J-V* curve of $FAPbI_3$ PSCs[54]

Chen等人[61]引入配位性更强的离子液体丙酸甲胺(MAPa)作为共溶剂, 通过在受限的介孔结构中形成溶剂挥发通道来促进MAAc分子的逸出, 从而实现了MAAc的完全挥发和钙钛矿晶体在介孔结构内的高填充度, 如图6(f)所示. 此外, MAPa还促进了钙钛矿晶体的垂直生长, 并与钙钛矿表面未结合的Pb^{2+}配位, 这有助于提高丝网印刷薄膜的电荷传输效率和界面能带对齐, 如图6(g)所示. 最后, 全丝网印刷PSCs的冠军PCE约为17%, 这是全丝网印刷PSCs的记录值, 如图6(h)所示.

离子液体在丝网印刷钙钛矿太阳能电池中的应用, 不仅提高了制造过程的可控性和适应性, 还显著提升了太阳能电池的性能, 为钙钛矿太阳能电池的商业化和大规模生产提供了有力的技术支持.

6 基于ILs获得高效稳定PSCs的机制

离子液体作为前驱体溶剂是PSCs的一项突破, 它使得通过简单的旋涂方法, 无需辅助溶剂即可制备出性能优异且在环境空气中长期稳定的PSCs. 此外, ILs作为溶剂, 在其他钙钛矿光电器件中也显示出巨大的优势, 包括发光二极管[62]、存储器[63]、荧光材料[64]、激光器[65]、光电探测器[66]等. 最近, 我们研究了ILs实现高效、稳定PSCs的作用机制, 并进一步提高了其性能. 在制备高效稳定的PSCs过程中, ILs可以同时发挥溶剂、添加剂和钝化等多种功能[23].

ILs可以通过溶剂与溶质之间独特的化学相互作用来溶解钙钛矿前驱体并获得长期稳定的钙钛矿胶体溶液[60]. MAAc通过Ac^-和Pb^{2+}之间的Pb···O配位以及NH_3^+和I^-之间的氢键, 获得了稳定且均匀分布的钙钛矿胶体[67], 如图7(a), (b)所示. 在传统的DMF/DMSO溶剂体系中, 钙钛矿胶束呈现出不规则取向的团簇片状结构. 而在MAAc溶剂中, 由于强配位相互作用和氢键的存在, 钙钛矿前驱体中的胶体形成了尺寸均匀、形状相似、取向规则、性质相同的均匀结构胶束, 如图7(c)所示, 这种均匀结构的稳定胶束有利于形成高质量

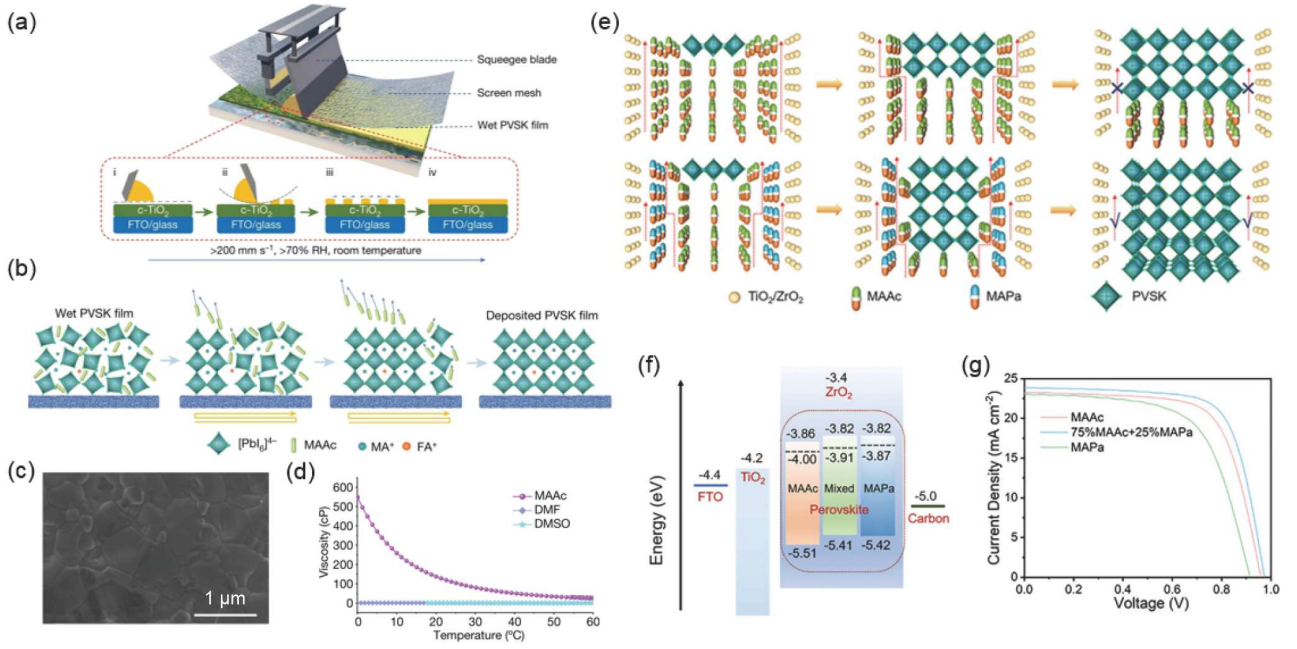

图 6 (网络版彩色)ILs用于制备全丝网印刷PSCs. (a) 丝网印刷方法沉积钙钛矿薄膜的示意图; (b) 湿钙钛矿薄膜的热退火沉积示意图; (c) 丝网印刷钙钛矿薄膜SEM图案; (d) MAAc、DMF和DMSO溶剂的温度和黏度之间的关系; (e) 丝网印刷PSCs的*J-V*曲线[59]; (f) 基于MAAc/MAPa溶剂体系的钙钛矿纳米晶体在介孔层中的生长过程示意图; (g) 不同溶剂的前驱体溶液制备的钙钛矿薄膜的能级图[61]

Figure 6 (Color online) ILs for the fabrication of fully screen-printed perovskite solar cells. (a) Diagram of the screen-printing method for the deposition of perovskite thin films; (b) schematic of the thermal annealing deposition of wet perovskite thin films; (c) SEM images of the perovskite thin films fabricated by screen-printing; (d) relationship between temperature and viscosity of MAAc, DMF and DMSO solvents; (e) *J-V* curve of $FAPbI_3$ PSCs[59]; (f) schematic illustration of the growth process of the perovskite nanocrystals in the mesoporous layer based on MAAc/MAPa solvent systems; (g) energy level diagrams of perovskite films prepared from precursor solutions in different solvents[61]

的钙钛矿薄膜.

在成膜过程中，MAAc摆脱了配位和氢键的束缚, 由于热应力而蒸发. 在这个过程中，I^-可以快速移动, 取代Ac^-的位置, 直接形成钙钛矿相, 如图7(d)所示. 这与传统的分子溶剂产生多种中间相再结晶不同[68]，如图7(e)，(f)所示. 从前驱体溶液到结晶的动力学过程如反应式(1)和(2)所示:

$$PbI_2 + CH_3NH_3I + CH_3COONHCH_3 \rightarrow Pb(CH_3COO)_2 \cdots CH_3NH_3I \quad (1)$$

$$Pb(CH_3COO)_2 \cdots CH_3NH_3I \rightarrow CH_3NH_3PbI_3 + CH_3COOH\uparrow + CH_3NH_2\uparrow \quad (2)$$

直接结晶过程可以有效抑制非钙钛矿相的形成和降低晶体缺陷态密度，显著提高了钙钛矿光伏器件的性能. 这些研究结果表明，MAAc不仅是一种出色的溶剂, 而且在钙钛矿器件的制备过程中, 作为调控结晶过程的添加剂也发挥着关键作用. 在以往的研究中, 通过将ILs作为独立添加剂来控制晶体生长，已经得到了多次验证[69~73]. 此外, MAAc的高沸点、低蒸汽压和强化学作用使其难以完全从薄膜中去除, 残留的MAAc主要分布在晶界而非晶格内部，如图7(g)所示. MAAc能够原位锚定钙钛矿八面体和未配位的Pb^{2+}，通过Pb···O配位作用抑制Pb^{2+}的迁移，并利用N-H···I氢键抑制I^-的迁移. 这些作用有助于减少钙钛矿材料的内部缺陷, 从而提高器件的稳定性. 经ILs处理的器件, 在连续光照超过5200 h后，仍能保持80%的初始性能[74,75]. 这一发现对于未来能源技术的应用具有重要意义. 为了进一步理解ILs的作用机制，需要深入的理论支持来系统设计具有不同功能的ILs. 这将为开发高效稳定的PSCs和推动钙钛矿光伏技术的大规模应用提供坚实的科学基础.

7 总结与展望

在本综述中，我们探讨了利用离子液体(ILs)制备钙钛矿太阳能电池(PSCs)的研究进展. 首先，探索了离子液体作为溶剂在PSCs中的应用. 通过采用离子液体MAAc作为溶剂，实现了在环境空气中无需反溶剂处

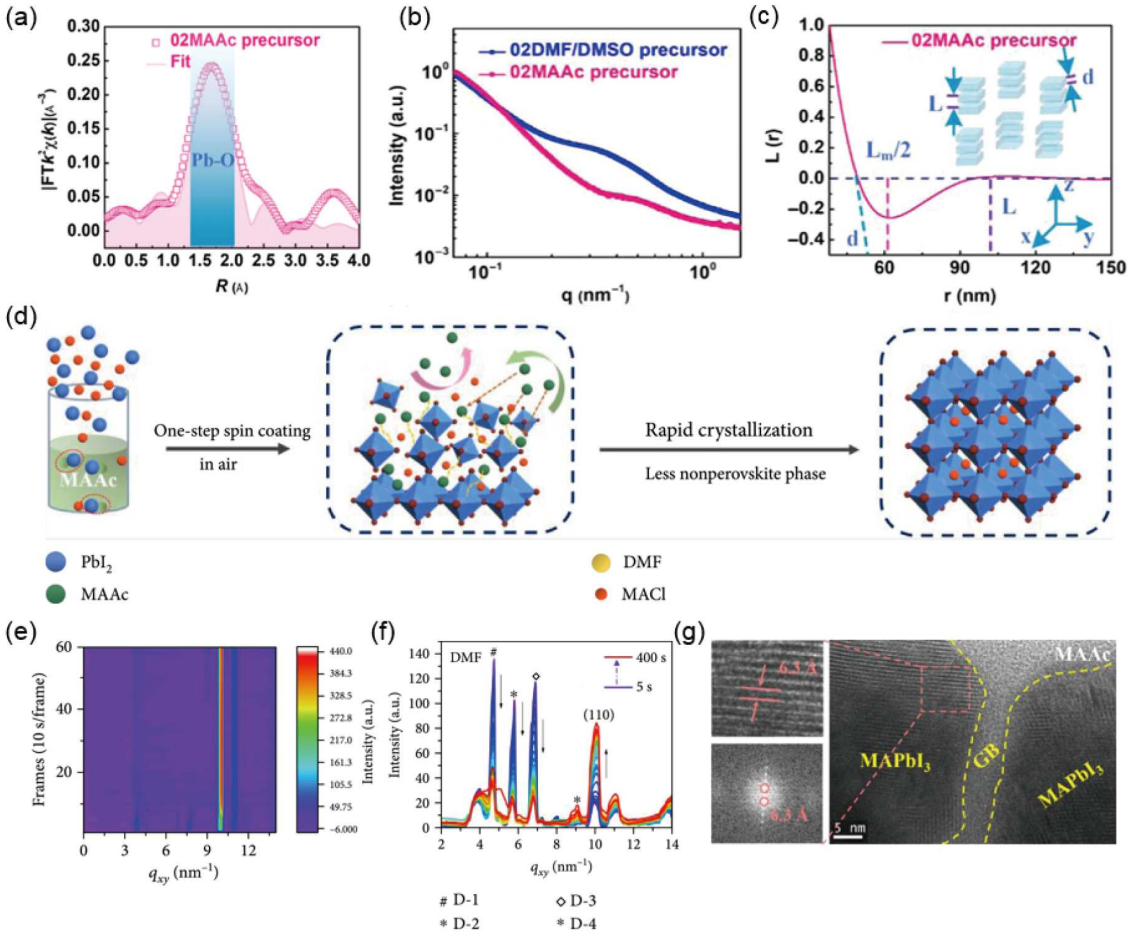

图 7 (网络版彩色)ILs获得高效稳定PSCs的机制. (a) 基于MAAc前驱体溶液的Pb L-III EXAFS光谱; (b) 钙钛矿前驱体胶体的SAXS强度图; (c) MAAc中的前驱体胶体分布拟合[67]; (d) MAAc中的钙钛矿晶体生长过程的机理图; (e) 基于MAAc钙钛矿的原位GIWAXS图像; (f) 基于DMF钙钛矿薄膜在q_{xy}方向上40帧(每帧10 s)的1D GIWAXS衍射图; (g) 基于MAAc钙钛矿薄膜的高分辨率透射电子显微镜[68]

Figure 7 (Color online) The mechanisms by which ILs achieve high-efficiency and stable perovskite solar cells. (a) The EXAFS spectra observed on the Pb L-III edge of the precursor solution prepared using MAAc; (b) perovskite precursor colloidal SAXS intensity; (c) fitting of the precursor colloidal distribution in MAAc[67]; (d) the diagram of the mechanism of the perovskite crystal growth process in MAAc; (e) *in-situ* GIWAXS images of perovskite based on MAAc; (f) 1D GIWAXS diffraction pattern of DMF thin films in the q_{xy} direction for 40 frames (10 s per frame); (g) The perovskite film was characterized by high-resolution transmission electron microscopy (HR-TEM)[68]

理即可通过一步法制备高质量钙钛矿薄膜. MAAc作为一种多功能溶剂, 能够制备包括有机-无机杂化钙钛矿、全无机钙钛矿、锡基钙钛矿以及二维层状钙钛矿在内的多种钙钛矿类型. 值得注意的是, 这些类型的钙钛矿具有优异的光伏性能, 并且完全在空气中制备. 此外, 通过界面改性、溶剂工程和添加剂工程等策略, 进一步提升了PSCs的效率与稳定性. 然后, 我们重点介绍了通过改变阴离子或阳离子的结构实现多功能应用的研究工作. 例如, 通过MAFa作为ILs溶剂, 在潮湿空气中成功制备了α-$FAPbI_3$钙钛矿, 并通过BAAc离子液体构建了纯相二维层状钙钛矿结构. 此外, ILs通过简化的制备工艺、提升薄膜质量、增强稳定性、适应多种制备技术和多功能性等多方面的优势, 为钙钛矿大规模制造提供了有力支持. 最后, 揭示了基于ILs的PSCs高效率和稳定性的根源. ILs通过其“三重功能”: 作为溶剂、添加剂和钝化剂, 实现了PSCs的高效性和长期运行稳定性. 首先, ILs通过杂化阴离子和阳离子与溶质之间的相互作用, 展现出高溶解度. 其次, ILs能够有效控制钙钛矿结晶的动力学过程, 从而制备出具有高取向性和高结晶度的高质量钙钛矿薄膜. 第三, 残留的ILs可以通过与钙钛矿原位相互作用来钝化晶界或表面.

尽管ILs在PSCs中展现出优异的性能, 但其在光伏

应用领域的认识仍处于初级阶段. 为了进一步挖掘ILs的潜力, 在此, 我们对钙钛矿光伏中ILs的未来发展提出了一些展望和可能的研究方向: (1) 利用ILs的阴离子和阳离子的混合结构, 通过改变阴离子或阳离子来调整其性质和功能, 全面控制钙钛矿的制备过程, 实现高性能PSCs. (2) 设计和合成具有还原性阳离子或阴离子的ILs溶剂, 以制备锡基或锡-铅混合PSCs, 避免引入额外的还原剂, 并解决锡基钙钛矿容易降解的问题. (3) 设计ILs的阴离子或阳离子为具有电荷传输功能的共轭结构, 为无需电荷传输层的高效稳定钙钛矿器件的制备提供新的可能性. (4) 利用ILs较大的黏度调节范围, 调节液体的流体力学特性, 以适应大面积模组制备.

钙钛矿光伏最终走向规模化生产. 无论钙钛矿体系如何, ILs都具有很大的优势, 包括简单的一步成膜、可调的黏度、节省原材料、可设计的结构. 我们坚信, 随着更多功能性ILs的合成和应用, 钙钛矿光伏技术将迎来新的发展机遇, 基于ILs的PSCs将在钙钛矿光伏技术中发挥关键作用.

参考文献

1 Stranks S D, Eperon G E, Grancini G, et al. Electron-hole diffusion lengths exceeding 1 micrometer in an organometal trihalide perovskite absorber. Science, 2013, 342: 341–344
2 Kojima A, Teshima K, Shirai Y, et al. Organometal halide perovskites as visible-light sensitizers for photovoltaic cells. J Am Chem Soc, 2009, 131: 6050–6051
3 Chen Y, Wu S, Li X, et al. Efficient and stable low-cost perovskite solar cells enabled by using surface passivated carbon as the counter electrode. J Mater Chem C, 2022, 10: 1270–1275
4 Liu S, Li J, Xiao W, et al. Buried interface molecular hybrid for inverted perovskite solar cells. Nature, 2024, 632: 536–542
5 Jung M, Ji S G, Kim G, et al. Perovskite precursor solution chemistry: from fundamentals to photovoltaic applications. Chem Soc Rev, 2019, 48: 2011–2038
6 Li B, Binks D, Cao G, et al. Engineering halide perovskite crystals through precursor chemistry. Small, 2019, 15: 1903613
7 Sharenko A, Mackeen C, Jewell L, et al. Evolution of iodoplumbate complexes in methylammonium lead iodide perovskite precursor solutions. Chem Mater, 2017, 29: 1315–1320
8 Ahn N, Son D Y, Jang I H, et al. Highly reproducible perovskite solar cells with average efficiency of 18.3% and best efficiency of 19.7% fabricated via lewis base adduct of lead(II) iodide. J Am Chem Soc, 2015, 137: 8696–8699
9 Lee J W, Dai Z, Lee C, et al. Tuning molecular interactions for highly reproducible and efficient formamidinium perovskite solar cells via adduct approach. J Am Chem Soc, 2018, 140: 6317–6324
10 Jo Y, Oh K S, Kim M, et al. High performance of planar perovskite solar cells produced from PbI_2 (DMSO) and PbI_2 (NMP) complexes by intramolecular exchange. Adv Mater Inter, 2016, 3: 1500768
11 Shen D, Yu X, Cai X, et al. Understanding the solvent-assisted crystallization mechanism inherent in efficient organic–inorganic halide perovskite solar cells. J Mater Chem A, 2014, 2: 20454–20461
12 Lv M, Dong X, Fang X, et al. A promising alternative solvent of perovskite to induce rapid crystallization for high-efficiency photovoltaic devices. RSC Adv, 2015, 5: 20521–20529
13 Noel N K, Habisreutinger S N, Wenger B, et al. A low viscosity, low boiling point, clean solvent system for the rapid crystallisation of highly specular perovskite films. Energy Environ Sci, 2017, 10: 145–152
14 Park N G. Green solvent for perovskite solar cell production. Nat Sustain, 2021, 4: 192–193
15 Wasserscheid P, Keim W. Ionic liquids—New “solutions” for transition metal catalysis. Angew Chem Int Ed, 2000, 39: 3772–3789
16 Shen M, Zhang Y, Chen K, et al. Ionicity of protic ionic liquid: quantitative measurement by spectroscopic methods. J Phys Chem B, 2017, 121: 1372–1376
17 Avilés M D, Pamies R, Sanes J, et al. Fatty acid-derived ionic liquid lubricant. Protic ionic liquid crystals as protic ionic liquid additives. Coatings, 2019, 9: 710
18 Xia R, Fei Z, Drigo N, et al. Retarding thermal degradation in hybrid perovskites by ionic liquid additives. Adv Funct Mater, 2019, 29: 1902021
19 Ghosh S, Singh T. Role of ionic liquids in organic-inorganic metal halide perovskite solar cells efficiency and stability. Nano Energy, 2019, 63: 103828
20 Moore D T, Tan K W, Sai H, et al. Direct crystallization route to methylammonium lead iodide perovskite from an ionic liquid. Chem Mater, 2015, 27: 3197–3199
21 Cho N, Li F, Turedi B, et al. Pure crystal orientation and anisotropic charge transport in large-area hybrid perovskite films. Nat Commun, 2016, 7:

13407
22 Chao L, Xia Y, Li B, et al. Room-temperature molten salt for facile fabrication of efficient and stable perovskite solar cells in ambient air. Chem, 2019, 5: 995–1006
23 Chao L, Niu T, Gu H, et al. Origin of high efficiency and long-term stability in ionic liquid perovskite photovoltaic. Research, 2020, 2020: 2020/2616345
24 Sun B, Wang W, Lu H, et al. Tuning the interactions of methylammonium acetate with acetonitrile to create efficient perovskite solar cells. J Phys Chem C, 2021, 125: 6555–6563
25 Fang M, Tao L, Wu W, et al. Residual solvent extraction via chemical displacement for efficient and stable perovskite solar cells. J Energy Chem, 2021, 61: 8–14
26 Wang W, Su Z, Sun B, et al. Toward efficient and stable perovskite solar cells by 2D interface energy band alignment. Adv Mater Inter, 2021, 8: 2001683
27 Razza S, Di Giacomo F, Matteocci F, et al. Perovskite solar cells and large area modules (100 cm^2) based on an air flow-assisted PbI_2 blade coating deposition process. J Power Sources, 2015, 277: 286–291
28 Gao L, Huang K, Long C, et al. Fully slot-die-coated perovskite solar cells in ambient condition. Appl Phys A, 2020, 126: 452
29 Li S G, Jiang K J, Su M J, et al. Inkjet printing of $CH_3NH_3PbI_3$ on a mesoscopic TiO_2 film for highly efficient perovskite solar cells. J Mater Chem A, 2015, 3: 9092–9097
30 Wang X, Ran X, Liu X, et al. Tailoring component interaction for air-processed efficient and stable all-inorganic perovskite photovoltaic. Angew Chem Int Ed, 2020, 59: 13354–13361
31 Wang Y, Dar M I, Ono L K, et al. Thermodynamically stabilized β-$CsPbI_3$–based perovskite solar cells with efficiencies >18%. Science, 2019, 365: 591–595
32 Xiang W, Wang Z, Kubicki D J, et al. Europium-doped $CsPbI_2Br$ for stable and highly efficient inorganic perovskite solar cells. Joule, 2019, 3: 205–214
33 Cui Y, Shi J, Meng F, et al. A versatile molten-salt induction strategy to achieve efficient $CsPbI_3$ perovskite solar cells with a high open-circuit voltage >1.2 V. Adv Mater, 2022, 34: 2205028
34 Aldibaja F K, Badia L, Mas-Marzá E, et al. Effect of different lead precursors on perovskite solar cell performance and stability. J Mater Chem A, 2015, 3: 9194–9200
35 Zhao L, Luo D, Wu J, et al. High-performance inverted planar heterojunction perovskite solar cells based on lead acetate precursor with efficiency exceeding 18%. Adv Funct Mater, 2016, 26: 3508–3514
36 Chen Y, Xu Y, Liu J, et al. A universal ionic liquid solvent for non-halide lead sources in perovskite solar cells. J Energy Chem, 2022, 71: 445–451
37 Ke W, Fang G, Wan J, et al. Efficient hole-blocking layer-free planar halide perovskite thin-film solar cells. Nat Commun, 2015, 6: 6700
38 Wu W, Liao J, Zhong J, et al. Suppressing interfacial charge recombination in electron-transport-layer-free perovskite solar cells to give an efficiency exceeding 21 %. Angew Chem Int Ed, 2020, 59: 20980–20987
39 Li D, Chao L, Chen C, et al. *In situ* interface engineering for highly efficient electron-transport-layer-free perovskite solar cells. Nano Lett, 2020, 20: 5799–5806
40 Chen H, Xia Y, Wu B, et al. Critical role of chloride in organic ammonium spacer on the performance of low-dimensional Ruddlesden-Popper perovskite solar cells. Nano Energy, 2019, 56: 373–381
41 Chao L, Niu T, Xia Y, et al. Efficient and stable low-dimensional Ruddlesden–Popper perovskite solar cells enabled by reducing tunnel barrier. J Phys Chem Lett, 2019, 10: 1173–1179
42 Zheng Y, Niu T, Qiu J, et al. Oriented and uniform distribution of Dion–Jacobson phase perovskites controlled by quantum well barrier thickness. Sol RRL, 2019, 3: 1900090
43 Ren H, Yu S, Chao L, et al. Efficient and stable Ruddlesden–Popper perovskite solar cell with tailored interlayer molecular interaction. Nat Photonics, 2020, 14: 154–163
44 Niu T, Ren H, Wu B, et al. Reduced-dimensional perovskite enabled by organic diamine for efficient photovoltaics. J Phys Chem Lett, 2019, 10: 2349–2356
45 Qiu J, Xia Y, Chen Y, et al. Management of crystallization kinetics for efficient and stable low-dimensional Ruddlesden–Popper (LDRP) lead-free perovskite solar cells. Adv Sci, 2019, 6: 1800793
46 Tsai H, Nie W, Blancon J C, et al. High-efficiency two-dimensional Ruddlesden–Popper perovskite solar cells. Nature, 2016, 536: 312–316
47 Tsai H, Asadpour R, Blancon J C, et al. Design principles for electronic charge transport in solution-processed vertically stacked 2D perovskite quantum wells. Nat Commun, 2018, 9: 2130
48 Chao L, Wang Z, Xia Y, et al. Recent progress on low dimensional perovskite solar cells. J Energy Chem, 2018, 27: 1091–1100
49 Liang C, Gu H, Xia Y, et al. Two-dimensional Ruddlesden–Popper layered perovskite solar cells based on phase-pure thin films. Nat Energy, 2021,

6: 38–45
50 McMeekin D P, Wang Z, Rehman W, et al. Crystallization kinetics and morphology control of formamidinium–cesium mixed-cation lead mixed-halide perovskite via tunability of the colloidal precursor solution. Adv Mater, 2017, 29: 1607039
51 Kim M, Kim G H, Lee T K, et al. Methylammonium chloride induces intermediate phase stabilization for efficient perovskite solar cells. Joule, 2019, 3: 2179–2192
52 Min H, Kim M, Lee S U, et al. Efficient, stable solar cells by using inherent bandgap of α-phase formamidinium lead iodide. Science, 2019, 366: 749–753
53 Hui W, Chao L, Lu H, et al. Stabilizing black-phase formamidinium perovskite formation at room temperature and high humidity. Science, 2021, 371: 1359–1364
54 Chao L, Xia Y, Duan X, et al. Direct and stable α-phase formation via ionic liquid solvation for formamidinium-based perovskite solar cells. Joule, 2022, 6: 2203–2217
55 Cheng Y B, Pascoe A, Huang F, et al. Print flexible solar cells. Nature, 2016, 539: 488–489
56 Hyun W J, Secor E B, Hersam M C, et al. High-resolution patterning of graphene by screen printing with a silicon stencil for highly flexible printed electronics. Adv Mater, 2015, 27: 109–115
57 Hu Y, Zhang Z, Mei A, et al. Improved performance of printable perovskite solar cells with bifunctional conjugated organic molecule. Adv Mater, 2018, 30: 1705786
58 Binyamin T, Etgar L. Ways to improve the performance of triple-mesoscopic hole-conductor-free perovskite-based solar cells. Sol RRL, 2022, 6: 2200295
59 Chen C, Chen J, Han H, et al. Perovskite solar cells based on screen-printed thin films. Nature, 2022, 612: 266–271
60 Wang X, Fan Y, Wang L, et al. Perovskite solution aging: what happened and how to inhibit? Chem, 2020, 6: 1369–1378
61 Chen C, Ran C, Guo C, et al. Fully screen-printed perovskite solar cells with 17% efficiency via tailoring confined perovskite crystallization within mesoporous layer. Adv Energy Mater, 2023, 13: 2302654
62 Du H, Hui W, Tang L, et al. Highly oriented perovskites for efficient light-emitting diodes with balanced charge transport. Org Electron, 2020, 77: 105529
63 Xia F, Xu Y, Li B, et al. Improved performance of $CH_3NH_3PbI_{3-x}Cl_x$ resistive switching memory by assembling 2D/3D perovskite heterostructures. ACS Appl Mater Interfaces, 2020, 12: 15439–15445
64 Hoang M T, Pham N D, Yang Y, et al. A facile, environmentally friendly synthesis of strong photo-emissive methylammonium lead bromide perovskite nanocrystals enabled by ionic liquids. Green Chem, 2020, 22: 3433–3440
65 Wang Z, Luo M, Liu Y, et al. Air-processed $MAPbBr_3$ perovskite thin film with ultrastability and enhanced amplified spontaneous emission. Small, 2021, 17: 2101107
66 Wang Q, Zhang G, Zhang H, et al. High-resolution, flexible, and full-color perovskite image photodetector via electrohydrodynamic printing of ionic-liquid-based ink. Adv Funct Mater, 2021, 31: 2100857
67 Gu H, Niu T, Zuo S, et al. Stable metal–halide perovskite colloids in protic ionic liquid. CCS Chem, 2022, 4: 3264–3274
68 Chao L, Niu T, Gao W, et al. Solvent engineering of the precursor solution toward large-area production of perovskite solar cells. Adv Mater, 2021, 33: 2005410
69 Zhang Y, Fei Z, Gao P, et al. A strategy to produce high efficiency, high stability perovskite solar cells using functionalized ionic liquid-dopants. Adv Mater, 2017, 29: 1702157
70 Wu Y, Xie F, Chen H, et al. Thermally stable $MAPbI_3$ perovskite solar cells with efficiency of 19.19% and area over 1 cm^2 achieved by additive engineering. Adv Mater, 2017, 29: 1701073
71 Seo J, Matsui T, Luo J, et al. Ionic liquid control crystal growth to enhance planar perovskite solar cells efficiency. Adv Energy Mater, 2016, 6: 1600767
72 Xia Y, Ran C, Chen Y, et al. Management of perovskite intermediates for highly efficient inverted planar heterojunction perovskite solar cells. J Mater Chem A, 2017, 5: 3193–3202
73 Zhang T, Wang Y, Wang X, et al. Organic salt mediated growth of phase pure and stable all-inorganic $CsPbX_3$ (X = I, Br) perovskites for efficient photovoltaics. Sci Bull, 2019, 64: 1773–1779
74 Bai S, Da P, Li C, et al. Planar perovskite solar cells with long-term stability using ionic liquid additives. Nature, 2019, 571: 245–250
75 Lin Y H, Sakai N, Da P, et al. A piperidinium salt stabilizes efficient metal-halide perovskite solar cells. Science, 2020, 369: 96–102

Summary for “离子液体介导的钙钛矿光伏电池”

Ionic liquids mediated perovskite photovoltaic cells

Wan Yang, Zihan Gu, Lingfeng Chao*, Yingdong Xia* & Yonghua Chen*

School of Flexible Electronics (Future Technologies), Institute of Advanced Materials (IAM), Nanjing Tech University (NanjingTech), Nanjing 210000, China

* Corresponding authors, E-mail: iamlfchao@njtech.edu.cn; iamydxia@njtech.edu.cn; iamyhchen@njtech.edu.cn

Ionic liquids (ILs) are a class of salts that remain liquid at room temperature and possess unique physical and chemical properties, making them highly promising for applications in perovskite solar cells (PSCs). ILs play a crucial role in enhancing the performance and stability of PSCs. This review systematically summarizes the research progress in fabricating PSCs using ILs as solvents. Initially, the application of ILs as solvents in PSCs is explored. By employing MAAc as a solvent, high-quality perovskite films can be fabricated through a one-step method in ambient air without the need for anti-solvent treatment. MAAc, a multifunctional solvent, enables the fabrication of various types of perovskites, including organic-inorganic hybrid, all-inorganic, tin-based, and two-dimensional layered perovskites. Notably, these perovskites exhibit excellent photovoltaic performance and are entirely fabricated in air. Furthermore, strategies such as interfacial modification, solvent engineering, and additive engineering are employed to further enhance the efficiency and stability of PSCs. Subsequently, the review highlights research that achieves multifunctionality by altering the structure of anions or cations. For instance, MAFa as an IL solvent successfully fabricates α-$FAPbI_3$ perovskites in humid air, and BAAc constructs pure-phase two-dimensional layered perovskite structures. Additionally, ILs offer multiple advantages through simplified fabrication processes, improved film quality, enhanced stability, adaptability to various fabrication techniques, and multifunctionality, providing strong support for the large-scale manufacturing of perovskites. Finally, the review reveals the roots of high efficiency and stability in IL-based PSCs. ILs function as solvents, additives, and passivators, contributing to the high efficiency and long-term operational stability of PSCs. First, ILs exhibit high solubility through interactions between hybrid anions and cations and the solute. Second, ILs effectively control the crystallization kinetics of perovskites, resulting in high-quality films with high orientation and crystallinity. Third, residual ILs passivate grain boundaries or surfaces through *in-situ* interactions with perovskites.

Although ILs have shown excellent performance in PSCs, their application in photovoltaics is still in its infancy. To further explore the potential of ILs, future research directions for ILs in perovskite photovoltaics are proposed: Adjust the properties and functions of ILs by altering anions or cations to control the perovskite fabrication process and achieve high-performance PSCs; Design and synthesize ILs with reducing cations or anions for tin-based or tin-lead mixed PSCs, avoiding additional reducing agents and addressing the degradation issue of tin-based perovskites; Design ILs with conjugated structures in anions or cations for efficient charge transport in PSCs without electron transport layers; Utilize the broad viscosity adjustment range of ILs to regulate the fluid dynamics of liquids for large-area module fabrication.

As perovskite photovoltaics move towards scaled production, ILs offer significant advantages, including simple one-step film formation, adjustable viscosity, material savings, and designable structures. We are confident that with the synthesis and application of more functional ILs, perovskite photovoltaic technology will usher in new development opportunities, and IL-based PSCs will play a crucial role in this field.

perovskite solar cells, ionic liquids, stability, large-area fabrication

doi: 10.1360/TB-2024-1310